AD-A045 160 PENNSYLVANIA STATE UNIV UNIVERSITY PARK APPLIED RESE--ETC F/G 17/1
DIRECTIONAL PATTERNS OF TRANSDUCER ARRAYS.(U)
JUL 77 P M KENDIG
UNCLASSIFIED TM-77-213 N00017-73-C-1418
NL

1 OF 1
AD
A045160

END
DATE
FILMED
11-77
DDC

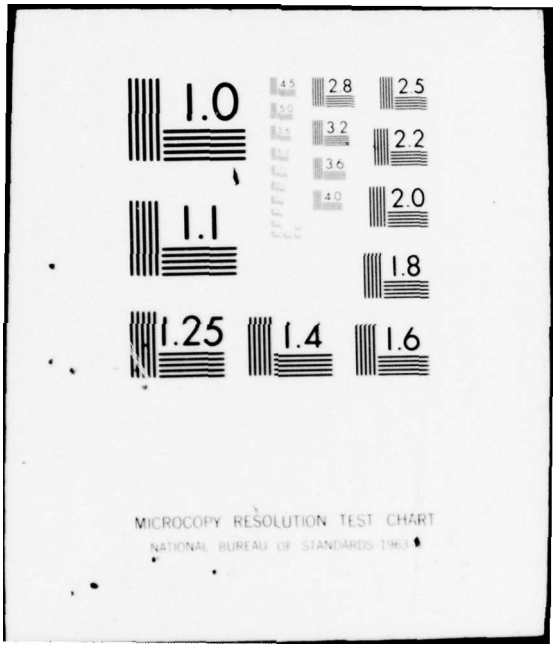
1.0
1.1
1.25
1.4
1.6
1.8
2.0
2.2
2.5
2.8
3.2
3.6
4.0
4.5
5.0
MICROCOPY RESOLUTION TEST CHART
NATIONAL BUREAU OF STANDARDS 1963

(12)

DIRECTIONAL PATTERNS OF TRANSDUCER ARRAYS

P. M. Kendig

Technical Memorandum
File No. TM 77-213
July 7, 1977
Contract N00017-73-C-1418

Copy No. 12

The Pennsylvania State University
Institute for Science and Engineering
APPLIED RESEARCH LABORATORY
P. O. Box 30
State College, PA 16801

NAVY DEPARTMENT

NAVAL SEA SYSTEMS COMMAND

UNCLASSIFIED

SECURITY CLASSIFICATION OF THIS PAGE (When Data Entered)

REPORT DOCUMENTATION PAGE		READ INSTRUCTIONS BEFORE COMPLETING FORM
1. REPORT NUMBER (14) TM-77-213	2. GOVT ACCESSION NO.	3. RECIPIENT'S CATALOG NUMBER
4. TITLE (and Subtitle) (6) DIRECTIONAL PATTERNS OF TRANSDUCER ARRAYS.		5. TYPE OF REPORT & PERIOD COVERED: Interim 6. PERFORMING ORG. REPORT NUMBER
7. AUTHOR(s) (10) P. M. Kendig		8. CONTRACT OR GRANT NUMBER(s) (15) N00017-73-C-1418
9. PERFORMING ORGANIZATION NAME AND ADDRESS Applied Research Laboratory P. O. Box 30 State College, PA 16801		10. PROGRAM ELEMENT, PROJECT, TASK AREA & WORK UNIT NUMBERS (12) 35 p.
11. CONTROLLING OFFICE NAME AND ADDRESS Naval Sea Systems Command Washington, DC 20362		12. REPORT DATE (11) July 7, 1977 13. NUMBER OF PAGES 29
14. MONITORING AGENCY NAME & ADDRESS (if different from Controlling Office) (9) Technical memo.		15. SECURITY CLASS. (of this report) UNCLASSIFIED 15a. DECLASSIFICATION/DOWNGRADING SCHEDULE

16. DISTRIBUTION STATEMENT (of this Report)

Approved for public release; distribution unlimited, per NAVSEA, June 1, 1977.

17. DISTRIBUTION STATEMENT (of the abstract entered in Block 20, if different from Report)

18. SUPPLEMENTARY NOTES

19. KEY WORDS (Continue on reverse side if necessary and identify by block number)

patterns
transducer arrays

20. ABSTRACT (Continue on reverse side if necessary and identify by block number)

The historical development of directional beam patterns of planar transducer arrays consisting of a relatively large number of electroacoustic transducing elements is outlined. Special attention is given to the Dolph-Chebyshev method of shading (tapering) the array elements to achieve minor lobe reduction. This method originally considered an array of uniformly spaced, coplanar elements that were all driven in phase; thus, giving a farfield directional beam normal to the plane of the array. When the constant phase

DD FORM 1 JAN 73 1473 EDITION OF 1 NOV 65 IS OBSOLETE

391 007

UNCLASSIFIED

SECURITY CLASSIFICATION OF THIS PAGE (When Data Entered)

20. Abstract (Cont'd)

requirement is relinquished, super directive, difference, and tilted beams including endfire arrays are achieved. Some attention is also given to the practical aspects of achieving the desired results. A brief discussion of parametric arrays is also given.

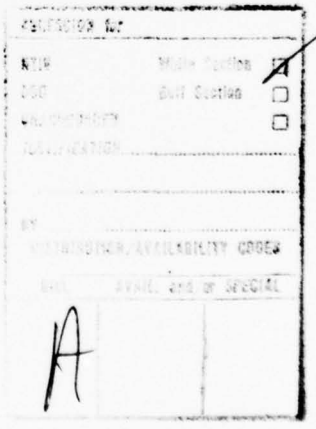

Subject: Directional Patterns of Transducer Arrays

Abstract: The historical development of directional beam patterns of planar transducer arrays consisting of a relatively large number of electroacoustic transducing elements is outlined. Special attention is given to the Dolph-Chebyshev method of shading (tapering) the array elements to achieve minor lobe reduction. This method originally considered an array of uniformly spaced, co-planar elements that were all driven in phase; thus, giving a farfield directional beam normal to the plane of the array. When the constant phase requirement is relinquished, super directive, difference, and tilted beams including endfire arrays are achieved. Some attention is also given to the practical aspects of achieving the desired results. A brief discussion of parametric arrays is also given.

TABLE OF CONTENTS

LIST OF FIGURES

The 93rd Meeting of the Acoustical Society of America Invited Paper KK3, 2 P.M., June 9, 1977. Directional Patterns of Transducer Arrays.
Paul M. Kendig, Applied Research Laboratory, Pennsylvania State University, University Park, Penna. 16802

In order to locate objects under water by means of sound waves, it is desirable to transmit sound in - or receive sound from - one principal direction. This is usually accomplished by employing an array of electro-acoustic transducer elements. If the object to be located is itself a source of sound, then only a receiving array (hydrophone) is required. If the object is not a self radiator of sound, then the array must transmit a sound pulse and determine the direction of the object from the direction of the returned echo. For this (the active case) the same array usually serves both functions, i.e., sound projector and receiving hydrophone. The range of the object may also be determined with the active system by measuring the travel time of the sound pulse to the target and back.

One characteristic of a reciprocal electroacoustic transducer (the type most commonly used) is that the directional responses or patterns are the same for both the transmitting and receiving modes. This is convenient because in the following discussion, it is not necessary to distinguish between the two modes because every thing that follows applies to both. The following discussion is given in greater detail in Reference 1.

A typical arrangement of transducer elements in a planar array is shown in Figure 1 where the small circles represent the locations of the centers of the radiating faces of the transducing elements. These are usually square or rectangular surfaces. The spacing of columns and rows are uniformly spaced but not necessarily equal to each other.

The directional pattern in a plane containing the x-axis is identical to that of a line parallel to the x-axis and with strengths equal to the sums of those in the respective columns. We can then determine this

specific pattern by reducing the problem to that of determining the pattern of a line of equally spaced sources. Of course, the same applies to a pattern in a plane that contains the y-axis.

A slight modification to the pattern obtained by treating the elements as point sources is due to the directional characteristics of the radiating faces of the elements themselves which are all assumed to be identical. The actual pattern is then the product of the pattern of one of the identical elements and the pattern of the line array of point sources (first product theorem).

For the same reasons that the pattern of the planar array in a plane parallel to either lines or rows reduce to that of a row of sources, the pattern of a rectangular source in a plane parallel to a side reduces to that of a line. Consequently, we shall first determine the pattern of a line source. Parenthetically, one should be reminded that directional patterns are simply diffraction patterns and as such are similar to much that we have learned in optics.

Figure 2 helps describe the terms used to determine the pattern of a line source in a plane that contains the line. It shows a plane wave approaching the line at an angle of θ with the normal to the line. The signal received at the incremental portion of the line dx leads the signal (reference phase) received at the origin by an angle ψ which is shown to be

$$\psi = \frac{2\pi x}{\lambda} \sin \theta = kx \sin \theta$$

where λ is the wavelength of the sound wave and x is the distance of the element measured from the origin.

The pattern response P_σ is given by

$$P_\sigma = Q \int_{-\ell/2}^{\ell/2} e^{i\,k\,x\,\sin\theta}\, dx$$

where Q is the source strength per unit length and ℓ is the length of the line. Integrating, we get

$$P_\sigma = Q\left[\frac{e^{i\,k\ell/2\,\sin\theta} - e^{-i\,k\ell/2\,\sin\theta}}{i\,k\,\sin\theta}\right]$$

which, from an identity expressing the sine of an angle in terms of exponentials, becomes

$$P_\sigma = Q\ell\left[\frac{\sin\frac{k\ell}{2}\sin\theta}{\frac{k\ell}{2}\sin\theta}\right] .$$

Let $u' = \frac{k\ell}{2}\sin\theta$. Then $P_\sigma = \frac{Q\ell\,\sin u'}{u'}$ (1)

which is just the same as the diffraction of a slit in optics.

An important relationship for a plane rectangular radiating surface is obtained in the case where the source strength $F(x,y) = f(x)\,g(y)$. In this case

$$P_\sigma = \iint F(x,y)\, e^{i\,k(x\cos\alpha + y\cos\beta)}\, dx\, dy$$

$$= \left[\int f(x)\, e^{i\,k\,x\cos\alpha}\, dx\right]\left[\int g(y)\, e^{i\,k\,y\cos\beta}\, dy\right] \qquad (2)$$

where α, β, ν are angles between direction of observation and the x, y and z axes, respectively.

This very important theorem states that if the source strength for a plane rectangular surface may be expressed as the product of a function $f(x)$ and a function $f(y)$, then the directional pattern is the product of two patterns in planes containing the normal to the surface and parallel to the x and y axes, respectively. The full significance of this theorem will appear later when we discuss rectangular arrays of elements.

Since we have already shown that patterns in the principal planes of a rectangular array of point sources can each be given by a line of point sources, we shall consider an equally spaced, in-phase line of sources. The symbols that shall be used for such arrays are shown in Figure 3. The incident sound wave meets the line array at the angle θ as shown. All phases shall be referenced to that of the signal received by an element at the origin whether one is actually there or not. Note the right-left symmetry of the signal amplitudes.

Figure 4 is a representation of the signals recieved by each of the elements in a six element line array where $u = \frac{\pi d}{\lambda} \sin \theta$. The vectors above the axis represent the signals received from the elements on the right and those below the axis, the signals from the left.

It is easily seen from Figure 4 that the sum pattern of the six element line source is given by,

$$P_{\sigma 6} = A_1 \cos u + A_2 \cos 3u + A_3 \cos 5u \qquad (3)$$

and that over the major lobe the phase of the entire line array is the same as that of the reference signal. As θ and consequently u increases, $P_{\sigma 6}$ will at one point become zero (a null in the pattern) and then the phase suddenly reverses to 180°. Further increases of θ and u produce more nulls and phase reversals.

Figure 4 also shows that the difference pattern is given by,

$$P_{\delta,6} = A_1 \sin u + A_2 \sin 3u + A_3 \sin 5u \quad .$$

In this case, we note that for small angles of incidence on the right the phase leads by 90° and on the left lags by 90°. Whereas the sum pattern is a maximum for $\theta = 0$, the difference pattern is a null.

Corresponding pattern functions for odd number of elements are:

$$P_{\sigma n} = A_0 + A_1 \cos 2u + A_2 \cos 4u + \ldots$$

$$P_{\delta n} = A_1 \sin 2u + A_2 \sin 4u + \ldots$$

The characteristics of $P_{\sigma,6}$ and $P_{\delta,6}$ are illustrated in Figure 5. The combined use of these patterns give the necessary information for locating underwater targets. Note that over a range of incident angles near 0°, the difference between the magnitudes of the sum and difference patterns increases nearly linearly with θ. If the difference pattern leads the sum pattern by 90°, the target is on the right and if it lags by 90°, the target is on the left. In practice, the difference pattern is usually phase shifted 90° so that it is in phase for targets on one side and out of phase for the other.

It must be emphasized that those phase relationships hold only over a relatively small range of incident angles on both sides of the normal. In the minor lobe regions we noted earlier that phase reversals occur as θ is varied and where they occur are not the same for both patterns. Consequently, minor lobes, unless drastically reduced, will give false information. For

these reasons and others, methods for reducing minor lobes have been developed which are known as tapering or shading the array. It consists of a systematic variation of the signal amplitude coefficients of the elements. The process will be illustrated by an application to the six element array illustrated above.

Note that the pattern function was given by

$$P_{\sigma 6} = A_1 \cos u + A_2 \cos 3u + A_3 \cos 5u \qquad (3)$$

which is a Fourier series. This suggested the use of a Fourier transform relating the source strengths of the array to the pattern function. In one application, an amplitude distribution was derived to provide the Gaussian pattern. In this case, the Fourier transform is itself a Gaussian function.

However, the most common method of tapering is that developed by Dolph (Reference 2) and generally known as the Dolph-Chebyshev method because it sets the pattern function above equal to an appropriate Chebyshev polynomial.

In Equation (3) above, we let $x = \cos u$ and then express the cosine functions in powers of x using Chebyshev polynomials. Thus, Equation (3) becomes

$$\begin{aligned} P_{\sigma,6} &= A_1 x + A_2(4x^3 - 3x) + A_3(16x^5 - 20x^3 + 5x) \\ &= 16A_3x^5 + (4A_2 - 20A_3)x^3 + (A_1 - 3A_2 + 5A_3)x \quad . \end{aligned} \qquad (4)$$

The use of Chebyshev polynomials above is somewhat trivial compared to the really significant use which is to set the array polynomial above equal to

the Chebyshev polynomial

$$T_5(x_o x) = 16x_o^5 x^5 - 20x_o^3 x^3 + 5x_o x \tag{5}$$

where $x_o > 1$ and is given by $x_o = \cosh\{\frac{1}{n} \cosh^{-1} r\}$ (6)

where $r = \frac{\text{major}}{\text{minor}}$ lobe ratio.

The amplitudes A_1, A_2 and A_3 are now easily calculated by equating coefficients of like powers of Equations (4) and (5).

Figure 6 illustrates the properties of the fifth degree Chebyshev polynomial which applies to the six element array. Over the range of $-1 \leq x_o x \leq 1$, the Chebyshev polynomial function ranges between ± 1 because in this range the function is limited to the cosine function. However, by extending the independent variable $x_o x$ beyond ± 1, the Chebyshev polynomials can take values to $\pm$ infinity. Thus, we can make $x_o x$ and consequently $T_5(x_o x)$ as large as possible. $T_5(x_o x)$ will then correspond to the peak or maximum of our response. On the other hand, the minor lobes will all be the same and equal to unity.

This design method is optimum in the sense that, for a given minor lobe reduction, one obtains the narrowest possible beamwidths for the equally spaced, in-phase elements at a given frequency. We design so that at $\theta = 90°$, the Chebyshev polynomial is of unity magnitude just beyond the last null.

There are relatively narrow limits on the range of element spacing. If the spacing is too large, e.g., greater than λ, a second major lobe would appear before $\theta = 90°$. Also, the method does not work if the spacing is much less than $\lambda/2$. For smaller spacings, a slightly different method

was introduced by Riblet (Reference 3) and extended by Pritchard (Reference 4). In this method which can be applied to an odd number of elements, a Chebyshev polynomial in terms of an angle $\phi = \frac{2\pi d}{\lambda} \sin\theta$ is used instead of $u = \frac{\pi d}{\lambda} \sin\theta$. This analysis leads to narrower patterns than those given by the Dolph-Chebyshev technique and are called super-directive arrays. However, as the spacing becomes smaller, some of the excitation amplitudes become negative, that is, out of phase with the others. For very small spacing, the sum is considerably less than the sum of absolute values. Smaller tolerances on the amplitudes are then generally required and over-all efficiency is decreased.

Some characteristics of the Dolph-Chebyshev patterns can be determined directly from the values of x_o, d and λ. Of course, the latter depends on the frequency. These characteristics are (1) maximum allowable spacing, and (2) beam width at any specified levels below the peak. These results are shown in Figure 7. Our experience with transducer elements cemented to a rubber pad and mounted in a housing showed that since there is a baffle effect that significantly reduces levels at incident angles beyond 70°, it was possible to design for the last minor lobe to occur around 70°. The dashed line indicates the extension of this tolerance.

We shall now illustrate the calculations of the excitation amplitudes for our six element array. If we design for a 30 dB minor lobe reduction, 20 log r will be set equal to 30, which gives $r = 31.6$. From Equation (6) we get a value of 1.35 for x_o. From Equations (4) and (5) we obtain the following values for A_N.

$A_1 = 15.60 \qquad A_2 = 10.70 \qquad A_3 = 4.66$

normalized $\quad A_1 = 1.000 \qquad A_2 = 0.685 \qquad A_3 = 0.298$

Figure 8 illustrates how these values are used to extend the line array design to that for a two dimensional array using Equation (2). Due to the symmetry, only one quadrant of the array is necessary. Figure 9 gives the normalized values for these elements. Frequently the outside corner element is deleted so as to confirm to a circular housing. The pattern deterioration is generally small but in any case its effect is easily calculated. The numbers in parentheses give one possible set of turns on magnetostrictive stacks or on the transformer secondaries used with electric coupled transducer elements.

The coefficients that provide an optimum sum pattern are unsuitable for an optimum difference pattern. In fact, they degrade the difference pattern. Consequently, the difference pattern must be independently optimized.

With a slight modification, the Dolph technique may be employed to optimize a difference pattern, i.e., where the two halves are in phase opposition. The difference pattern function,

$$P_{\delta,6} = A_1 \sin u + A_2 \sin 3u + A_3 \sin 5u$$

may be expanded in terms of $\sin u$ as follows:

$$P_{\delta,6} = A_1 \sin u + A_2(3 \sin u - 4 \sin^3 u) + A_3(5 \sin u - 20 \sin^3 u + 16 \sin^5 u)$$

Now, if we divide by $\sin u$, we get,

$$\frac{P_{\delta,6}}{\sin u} = A_1 + A_2(3 - 4 \sin^2 u) + A_3(5 - 20 \sin^2 u + 16 \sin^4 u) \quad .$$

If we substitute $1 - \cos^2 u$ for $\sin^2 u$ and x for $\cos u$, the expression

above becomes,

$$\frac{P_{\delta,6}}{\sin u} = (A_1 - A_2 + A_3) + (4A_2 - 12A_3)\, x^2 + 16A_3 x^4 \quad .$$

We now equate this relationship to a 4th degree Chebyshev polynomial and proceed as before with the sum pattern. Please recall, however, that we used a 5th degree polynomial for the sum pattern. Also, note that since $P_{\delta,6} = \sin u\, T_4(x_o x)$, it is zero at $\theta = 0$ and then the absolute value increases rapidly for moderately small values of θ on both sides of zero.

The use of Equation (2) to extend the line array to a plane is shown in Figure 10. Here, the B factors are just the excitation coefficients for an optimum sum pattern. In fact, if all elements were connected in phase, we would obtain an optimum vertical sum pattern, but when the right and left halves are connected in phase opposition, we obtain the optimum horizontal difference pattern.

Figure 11 gives relative source amplitudes for the optimum difference pattern. The distinct difference between these coefficients and those for the sum pattern is quite evident by noting that the elements in the second column now have the greatest excitation instead of the first column as in the case of the sum pattern.

No direct method of finding x_o was available for the difference pattern but minor lobe reductions could be calculated for assumed values of x_o (see Reference 1) and plotted as shown in Figure 12. Thus, these plots permit us to select the appropriate x_o for a given minor lobe reduction.

Figure 5 presents a linear plot of the optimum sum and difference patterns. When this method for the optimum difference pattern was developed, it appeared that it would apply only to an even number of array columns. However, Geoffrey Wilson (Reference 5) has shown that it can be applied to

an odd number of columns, in which case the central column simply is not used to form the difference pattern.

Figure 13 is of academic interest. It represents the locus of the resultant signal from 1/2 of a transducer designed for (a) an optimum sum pattern and (b) an optimum difference pattern. It is the resultant of the vectors shown in Figure 4. The sum pattern response is the projection on the x-axis and that of the difference pattern is the projection on the y-axis. It clearly shows why the minor lobes are so small.

Tilted beams and end-fire arrays are obtained by introducing delay lines or phase shift networks into the circuits of each element or maybe column or row of the array so that for a given specified direction, the outputs of signals (including delays or phase shifts) will be in phase. The tapering procedures are generally similar to those described earlier.

Most of the development for end-fire arrays (beam tilted to 90°) resulted in superdirective arrays with some characteristics similar to those of Riblet (Reference 3) and Pritchard (Reference 4).

A somewhat different approach to the production of tilted sum and difference patterns was developed by W. J. Hughes and W. Thompson, Jr. (Reference 6). I shall demonstrate its use by an application to a tilted sum pattern which may be written,

$$P_\sigma = A_1 \cos(u - \phi) + A_2 \cos 3(u - \phi) + A_3 \cos 5(u - \phi) + \ldots$$

where ϕ is the required phase delay for elements on one side of center and phase advance for elements on the other side. Using the trigonometric identity for the cosine of the difference of two angles, the equation above becomes,

$$P_\sigma = [A_1 \cos \phi \cos u + A_2 \cos 3\phi \cos 3u + A_3 \cos 5\phi \cos 5u + \ldots]$$
$$+ [A \sin \phi \sin u + A_2 \sin 3\phi \sin 3u + A_3 \sin 5\phi \sin 5u + \ldots] .$$

Now for a given tilt angle ϕ, the sines and cosines involving ϕ are constants. Therefore, the pattern function becomes

$$P_\sigma = [A_1' \cos u + A_2' \cos 3u + A_3' \cos 5u + \ldots]$$
$$+ [A_1'' \sin u + A_2'' \sin 3u + A_3'' \sin 5u + \ldots]$$

where $A_n' = A_n \cos \phi$, and $A_n'' = A_n \sin \phi$, etc.

We note that P_σ is now the sum of a sum pattern and a difference pattern. Since the latter is in phase quadrature with the former, it must be shifted 90° before combining the two. Although the method is applicable to any values of A_m, tapering is easily achieved. The unprimed A_n coefficients are determined as before by using Chebyshev polynomials. The Hughes - Thompson technique is also applicable to tilted, difference patterns and end fire arrays. It is interesting to note that all pattern tapering techniques discussed so far have used Chebyshev polynomials.

An array tapering for an entirely different purpose was developed by W. J. Trott (Reference 7). Its purpose was to provide plane waves in a region of the near field of a relatively large array in order to calibrate transducers in the near field.

It is well known that the intensity along the axis of a circular radiating piston whose diameter is large compared to the wavelength has numerous maxima and minima (actually nulls) in the near field. It is also known that the total number of side lobes appearing in the far field is just twice the number of maxima which occur directly in front of the piston.

The above remarks suggest that if minor lobes are eliminated or greatly reduced, this axial variation should likewise be eliminated or reduced. Indeed this is the case. Applying these principles, Trott adjusted the excitation amplitudes of a large array of elements in order to provide an essentially plane wave region directly in front of the array. In his example, a 100 cm diameter array provided a cylindrical space in front of the array about 50 cm in diameter and about the same in length wherein there were plane waves.

Although it was not expressly stated, all the previous discussion was based on linear acoustic waves. When very intense, so-called finite sound waves are projected, non-linear or distorted waves are produced with a whole host of interesting properties. For example, if two pure tones are projected into the same medium, harmonics of the waves are produced, as well as sum and difference frequency waves. The highly directive character of these difference frequency beams was first recognized by Peter J. Westervelt (Reference 8).

In the following discussion we are primarily interested in the difference frequency that develops in the projected acoustic field. Usually the frequencies of the high intensity primary waves are close together so that the difference frequency is much smaller, say one-tenth or less.

When the near field primary wave absorption is quite small, the interaction zone will extend beyond the mean Rayleigh distance r_o . The interaction zone is that region in front of the transducer face where wave distortion occurs and acoustical energy is pumped from the primary waves into the distortion waves, including the difference frequency wave. Since this latter is of much lower frequency than any of the other waves and consequently attenuated much less than the others, it usually will be transmitted to greater ranges than the others even though its equivalent field pressure is much below that of the primary waves. The so-called

pumping occurs until the spreading loss of the primary waves reduce the intensity to such a level that distortion no longer exists. Since the virtual sources that produce the difference frequencies are essentially limited to the main beams of the primary waves, the low frequency difference pattern will be essentially the same as those of the much higher frequency primary patterns or even a little sharper. In fact, its far field directivity response is essentially equal to the product of the directivity responses of the primary patterns. One very important consequence of this is the almost total absence of minor lobes in the difference frequency pattern.

In order to achieve the same directivity with a conventional source operating at the difference frequency, the source diameter would have to exceed the diameter of the parametric array by the ratio of the mean primary frequency to the difference frequency.

The bandwidth of the difference frequencies may be very broad because it is really determined by the Q of the transducer that projects the primary waves.

Somewhat similarly, difference frequency waves can be produced which have a constant beam width over very wide frequency bands (e.g., greater than two octaves). Of course, sum, difference and tilted beams can be produced.

When the absorption coefficient of the primary waves is large, the attenuation may be so great that all of the interaction may take place within the near-field of the transducer, i.e., at ranges less than r_o. In this case, the interaction is essentially confined to a cylinder whose diameter is that of the transducer radiating face and of length roughly determined by the absorption coefficient. This interaction zone is really an extension of the source itself. Indeed, the beam-width of this virtual

end-fire array is given by the same relationship as that for an end-fire array and is always less than that for the "spreading-loss-limited" case.

Parametric receiving arrays are formed in a fluid by projecting a finite-amplitude "pump wave" into the medium to serve as a "carrier" for the weak incoming signal whose frequency equals the difference frequency of the transmitted waves.

REFERENCES

1. V. M. Albers, Underwater Acoustics Handbook II, The Pennsylvania State University Press, University Park, Penna., 1965.

2. C. L. Dolph, Inst. Radio Engrs. 34, 335-348, 1946.

3. H. J. Riblet, Proc. Inst. Radio Engrs. 35, 489-492, 1947.

4. R. L. Pritchard, J. Acoust. Soc. Am. 25, 879-891, 1953.

5. G. L. Wilson, J. Acoust. Soc. Am. 34, 915, 1966.

6. W. J. Hughes and W. Thompson, Jr., J. Acoust. Soc. Am. 59, 1040-1045, 1976.

7. W. J. Trott, J. Acoust. Soc. Am. 36, 1557-1568, 1964.

8. P. J. Westervelt, J. Acoust. Soc. Am. 32, 934, 1960.

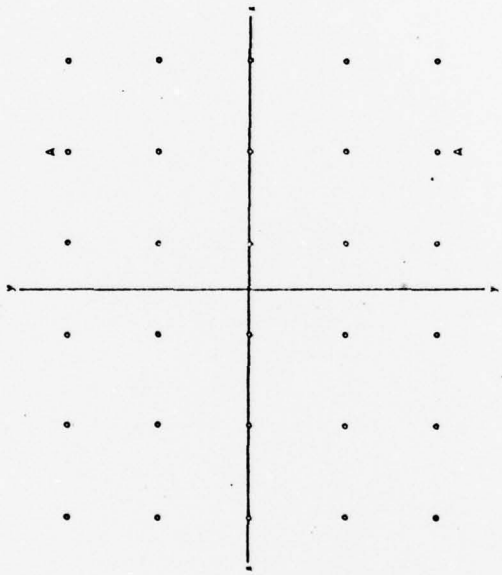

Figure 1 - Plane array of point sources showing the arrangement in rows and columns.

LINE SOURCE

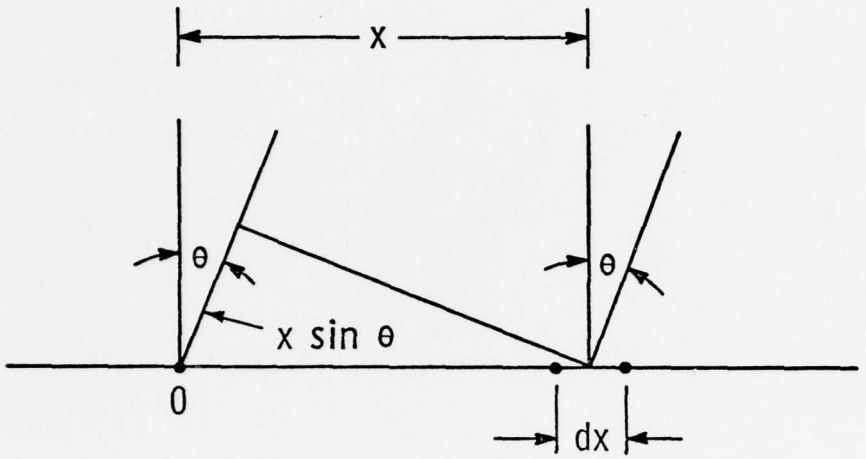

$$\psi = \frac{2\pi x}{\lambda} \sin\theta = kx \sin\theta$$

ψ: PHASE
λ: WAVELENGTH

Figure 2

July 7, 1977
PMK:cdn

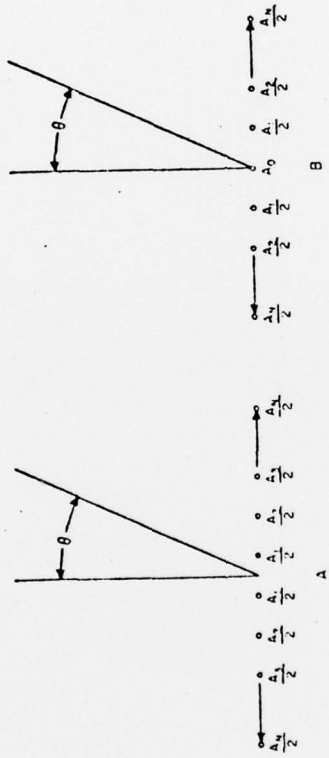

Figure 3 - Symbols for equally spaced linear arrays of point sources; (A) even number of sources, (B) odd number of sources.

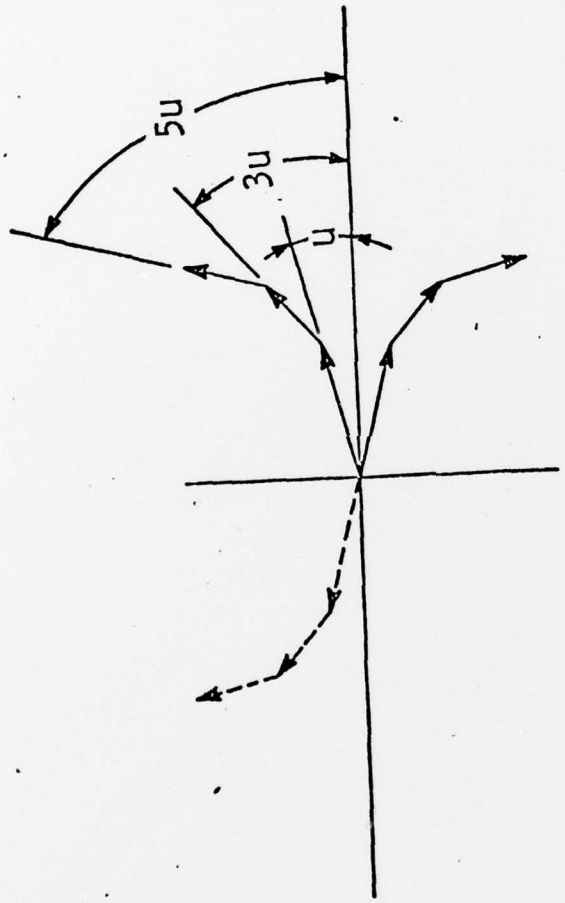

Figure 4. Vector Representation of Sum and Difference Responses

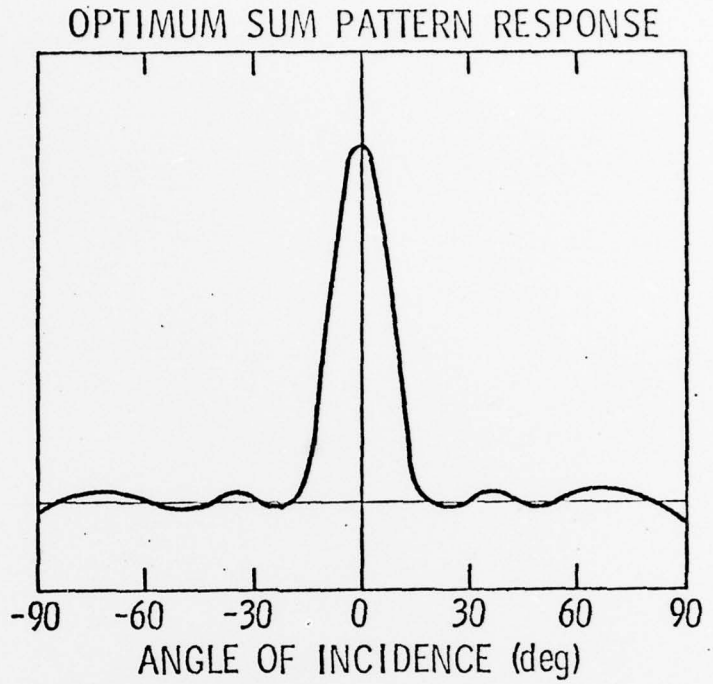

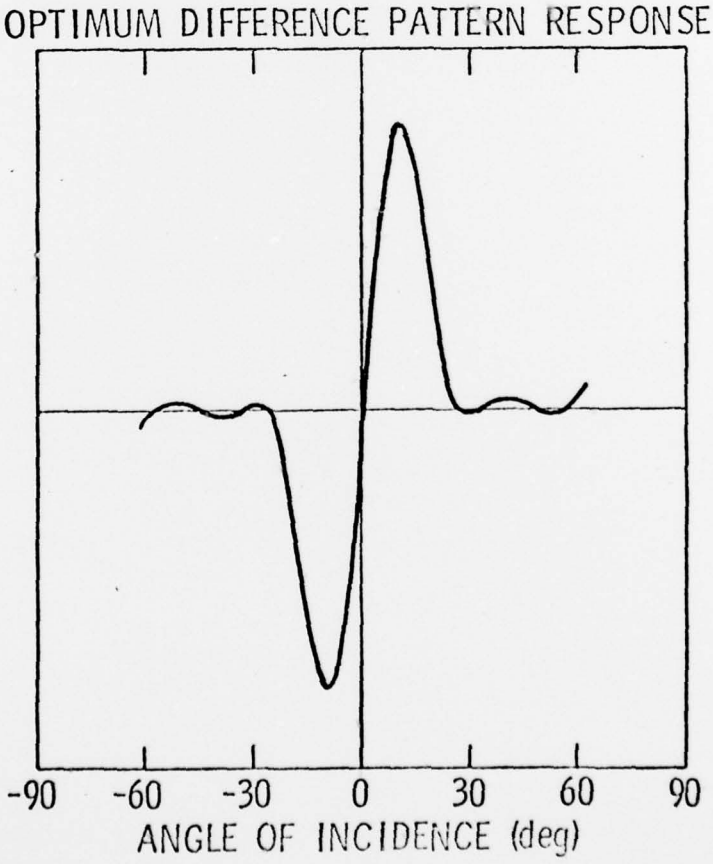

Figure 5 - Sum and difference responses

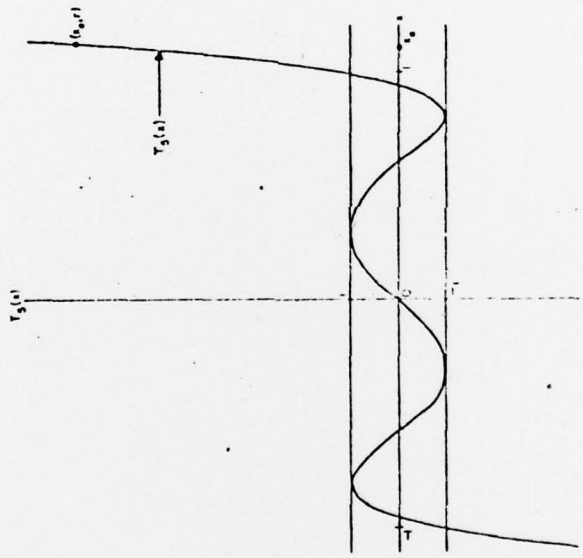

Figure 6 - Fifth Chebyshev polynomial showing relationship between signal to noise ratio r and parameter x_0.

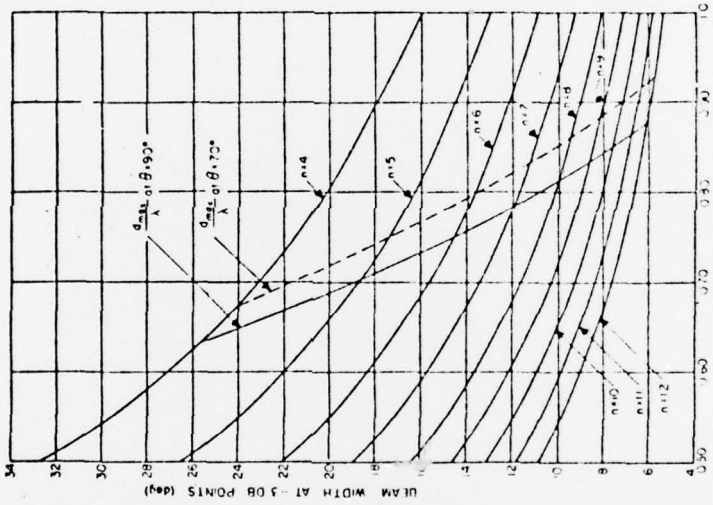

Figure 7 - Beam width vs. spacing for 30 db minor lobe reduction.
Parameter: number of elements.

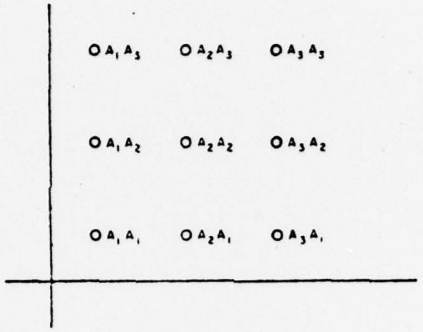

Figure 8 - Use of second product theorem to determine source amplitudes for a plane array sum pattern.

July 7, 1977
PMK:cdn

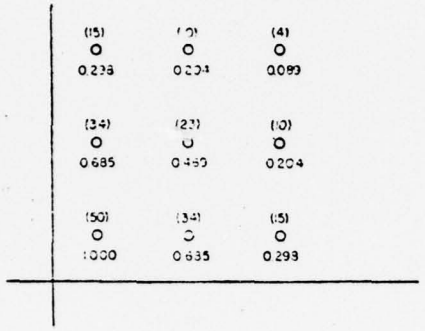

Figure 9 - Relative source amplitudes for a plane array designed for an optimum sum pattern. Numbers in parenthesis give one possible set of values for turns on magnetostrictive stacks.

July 7, 1977
PMK:cdn

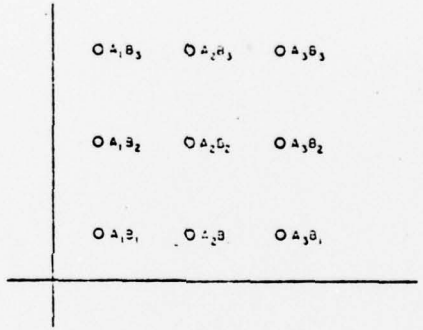

Figure 10 - Use of second-product theorem to determine source amplitudes for the difference pattern of a plane array.

(8) 0 0.69	(15) 0 0.268	(7) 0 0.142
(20) 0 0.39	(34) 0 0.635	(6) 0 0.326
(28) 0 0.571	(50) 0 1.000	(24) 0 0.477

Figure 11 - Relative source amplitudes for a plane array designed for an optimum difference pattern. Numbers in parenthesis give one possible set of values for the turns on magnetostrictive stacks.

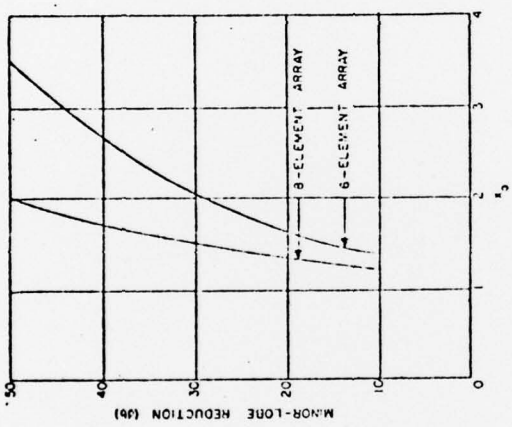

Figure 12 - Maximum minor lobe level relative to the level of the main beams for optimum difference patterns of six and eight element line arrays.

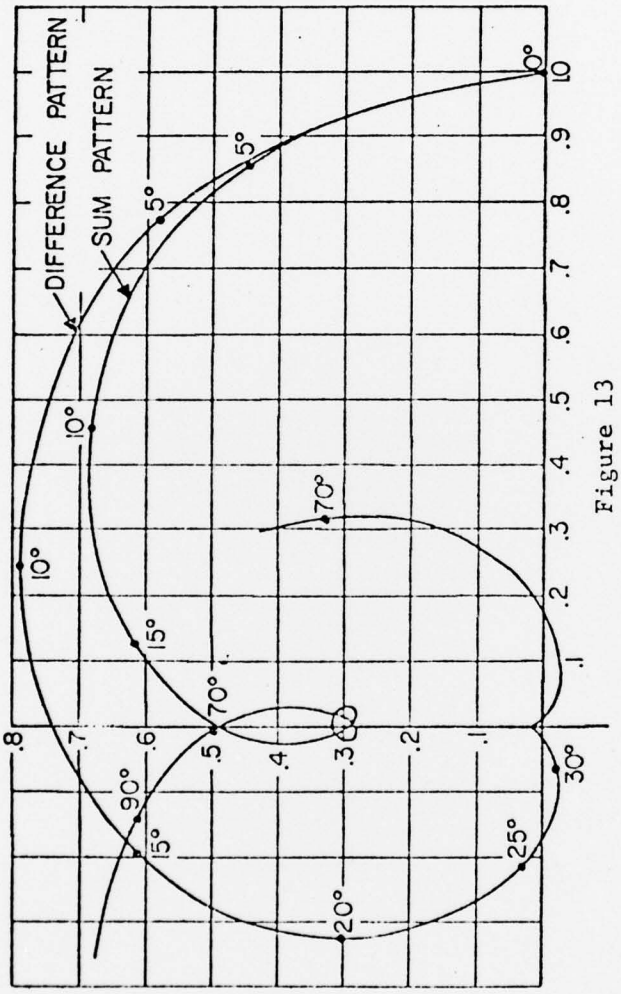

Figure 13

LOCUS OF VECTOR REPRESENTING THE SIGNAL FROM A HALF TRANSDUCER DESIGNED FOR (a) AN OPTIMUM SUM PATTERN AND (b) AN OPTIMUM DIFFERENCE PATTERN.

DISTRIBUTION LIST -- TM 77-213

NAVSEA, Dr. E. G. Liszka, SEA-03421, Copy No. 1
NAVSEA, Mr. T. E. Douglass, PMS 406E1, Copy No. 2
DDR&E, Dr. E. J. McKinney, Copy No. 3
NAVSEA, Code SEA-09G32, Copies No. 4 and 5
Picker Corp., 12 Clintonville Rd, Northford, CT 06472,
Mr. R. B. Bernardi, Copy No. 6
DDC, Copies No. 7 through 18

AD-A045 160 PENNSYLVANIA STATE UNIV UNIVERSITY PARK APPLIED RESE--ETC F/G 17/1
DIRECTIONAL PATTERNS OF TRANSDUCER ARRAYS.(U)
JUL 77 P M KENDIG N00017-73-C-1418

UNCLASSIFIED TM-77-213 NL

1 OF 1
AD
A045160

END
DATE
FILMED
11-77
DDC

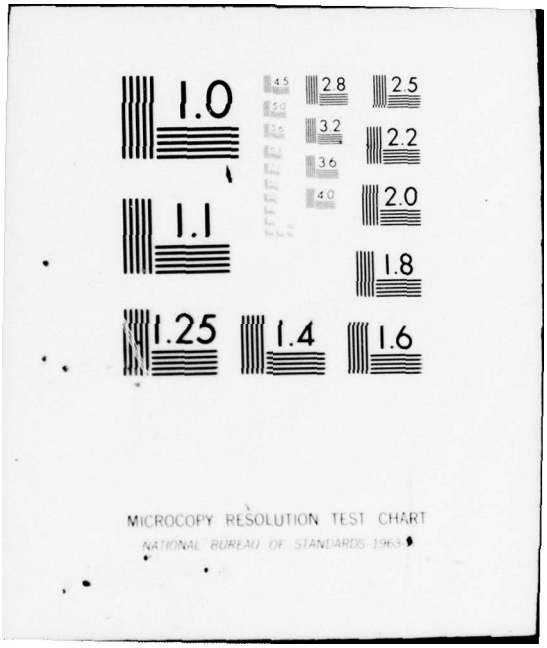
1.0
1.1
1.25
1.4
1.6
1.8
2.0
2.2
2.5
2.8
3.2
3.6
4.0
4.5
5.0
5.6
MICROCOPY RESOLUTION TEST CHART
NATIONAL BUREAU OF STANDARDS-1963

(12)

DIRECTIONAL PATTERNS OF TRANSDUCER ARRAYS

P. M. Kendig

Technical Memorandum
File No. TM 77-213
July 7, 1977
Contract N00017-73-C-1418

Copy No. 12

The Pennsylvania State University
Institute for Science and Engineering
APPLIED RESEARCH LABORATORY
P. O. Box 30
State College, PA 16801

NAVY DEPARTMENT

NAVAL SEA SYSTEMS COMMAND

UNCLASSIFIED

SECURITY CLASSIFICATION OF THIS PAGE *(When Data Entered)*

REPORT DOCUMENTATION PAGE	READ INSTRUCTIONS BEFORE COMPLETING FORM
1. REPORT NUMBER (14) TM-77-213	2. GOVT ACCESSION NO. / 3. RECIPIENT'S CATALOG NUMBER
4. TITLE *(and Subtitle)* (6) DIRECTIONAL PATTERNS OF TRANSDUCER ARRAYS	5. TYPE OF REPORT & PERIOD COVERED: Interim
	6. PERFORMING ORG. REPORT NUMBER
7. AUTHOR(s) (10) P. M. Kendig	8. CONTRACT OR GRANT NUMBER(s) (15) N00017-73-C-1418
9. PERFORMING ORGANIZATION NAME AND ADDRESS Applied Research Laboratory P. O. Box 30 State College, PA 16801	10. PROGRAM ELEMENT, PROJECT, TASK AREA & WORK UNIT NUMBERS (12) 35 p.
11. CONTROLLING OFFICE NAME AND ADDRESS Naval Sea Systems Command Washington, DC 20362	12. REPORT DATE (11) July 7, 1977 13. NUMBER OF PAGES 29
14. MONITORING AGENCY NAME & ADDRESS *(if different from Controlling Office)* (9) Technical memo.	15. SECURITY CLASS. *(of this report)* UNCLASSIFIED 15a. DECLASSIFICATION/DOWNGRADING SCHEDULE

16. DISTRIBUTION STATEMENT *(of this Report)*

Approved for public release; distribution unlimited, per NAVSEA, June 1, 1977.

17. DISTRIBUTION STATEMENT *(of the abstract entered in Block 20, if different from Report)*

18. SUPPLEMENTARY NOTES

19. KEY WORDS *(Continue on reverse side if necessary and identify by block number)*

patterns
transducer arrays

20. ABSTRACT *(Continue on reverse side if necessary and identify by block number)*

The historical development of directional beam patterns of planar transducer arrays consisting of a relatively large number of electroacoustic transducing elements is outlined. Special attention is given to the Dolph-Chebyshev method of shading (tapering) the array elements to achieve minor lobe reduction. This method originally considered an array of uniformly spaced, coplanar elements that were all driven in phase; thus, giving a farfield directional beam normal to the piane of the array. When the constant phase

DD FORM 1 JAN 73 1473 EDITION OF 1 NOV 65 IS OBSOLETE

391 007

UNCLASSIFIED

SECURITY CLASSIFICATION OF THIS PAGE *(When Data Entered)*

20. Abstract (Cont'd)

requirement is relinquished, super directive, difference, and tilted beams including endfire arrays are achieved. Some attention is also given to the practical aspects of achieving the desired results. A brief discussion of parametric arrays is also given.

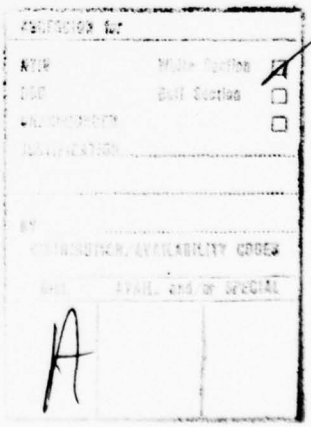

Subject: Directional Patterns of Transducer Arrays

Abstract: The historical development of directional beam patterns of planar transducer arrays consisting of a relatively large number of electroacoustic transducing elements is outlined. Special attention is given to the Dolph-Chebyshev method of shading (tapering) the array elements to achieve minor lobe reduction. This method originally considered an array of uniformly spaced, co-planar elements that were all driven in phase; thus, giving a farfield directional beam normal to the plane of the array. When the constant phase requirement is relinquished, super directive, difference, and tilted beams including endfire arrays are achieved. Some attention is also given to the practical aspects of achieving the desired results. A brief discussion of parametric arrays is also given.

TABLE OF CONTENTS

LIST OF FIGURES

The 93rd Meeting of the Acoustical Society of America Invited Paper KK3, 2 P.M., June 9, 1977. Directional Patterns of Transducer Arrays.
Paul M. Kendig, Applied Research Laboratory, Pennsylvania State University, University Park, Penna. 16802

In order to locate objects under water by means of sound waves, it is desirable to transmit sound in - or receive sound from - one principal direction. This is usually accomplished by employing an array of electro-acoustic transducer elements. If the object to be located is itself a source of sound, then only a receiving array (hydrophone) is required. If the object is not a self radiator of sound, then the array must transmit a sound pulse and determine the direction of the object from the direction of the returned echo. For this (the active case) the same array usually serves both functions, i.e., sound projector and receiving hydrophone. The range of the object may also be determined with the active system by measuring the travel time of the sound pulse to the target and back.

One characteristic of a reciprocal electroacoustic transducer (the type most commonly used) is that the directional responses or patterns are the same for both the transmitting and receiving modes. This is convenient because in the following discussion, it is not necessary to distinguish between the two modes because every thing that follows applies to both. The following discussion is given in greater detail in Reference 1.

A typical arrangement of transducer elements in a planar array is shown in Figure 1 where the small circles represent the locations of the centers of the radiating faces of the transducing elements. These are usually square or rectangular surfaces. The spacing of columns and rows are uniformly spaced but not necessarily equal to each other.

The directional pattern in a plane containing the x-axis is identical to that of a line parallel to the x-axis and with strengths equal to the sums of those in the respective columns. We can then determine this

specific pattern by reducing the problem to that of determining the pattern of a line of equally spaced sources. Of course, the same applies to a pattern in a plane that contains the y-axis.

A slight modification to the pattern obtained by treating the elements as point sources is due to the directional characteristics of the radiating faces of the elements themselves which are all assumed to be identical. The actual pattern is then the product of the pattern of one of the identical elements and the pattern of the line array of point sources (first product theorem).

For the same reasons that the pattern of the planar array in a plane parallel to either lines or rows reduce to that of a row of sources, the pattern of a rectangular source in a plane parallel to a side reduces to that of a line. Consequently, we shall first determine the pattern of a line source. Parenthetically, one should be reminded that directional patterns are simply diffraction patterns and as such are similar to much that we have learned in optics.

Figure 2 helps describe the terms used to determine the pattern of a line source in a plane that contains the line. It shows a plane wave approaching the line at an angle of θ with the normal to the line. The signal received at the incremental portion of the line dx leads the signal (reference phase) received at the origin by an angle ψ which is shown to be

$$\psi = \frac{2\pi x}{\lambda} \sin \theta = kx \sin \theta$$

where λ is the wavelength of the sound wave and x is the distance of the element measured from the origin.

The pattern response P_σ is given by

$$P_\sigma = Q \int_{-\ell/2}^{\ell/2} e^{i\,k\,x\,\sin\theta}\, dx$$

where Q is the source strength per unit length and ℓ is the length of the line. Integrating, we get

$$P_\sigma = Q\left[\frac{e^{i\,k\ell/2\,\sin\theta} - e^{-i\,k\ell/2\,\sin\theta}}{i\,k\,\sin\theta}\right]$$

which, from an identity expressing the sine of an angle in terms of exponentials, becomes

$$P_\sigma = Q\ell\left[\frac{\sin\frac{k\ell}{2}\sin\theta}{\frac{k\ell}{2}\sin\theta}\right] .$$

Let $u' = \frac{k\ell}{2}\sin\theta$. Then $P_\sigma = \frac{Q\ell\,\sin u'}{u'}$ (1)

which is just the same as the diffraction of a slit in optics.

An important relationship for a plane rectangular radiating surface is obtained in the case where the source strength $F(x,y) = f(x)\,g(y)$. In this case

$$P_\sigma = \int\int F(x,y)\, e^{i\,k(x\cos\alpha + y\cos\beta)}\, dx\, dy$$

$$= \left[\int f(x)\, e^{i\,k\,x\cos\alpha}\, dx\right]\left[\int g(y)\, e^{i\,k\,y\cos\beta}\, dy\right] \qquad (2)$$

where α, β, ν are angles between direction of observation and the x, y and z axes, respectively.

This very important theorem states that if the source strength for a plane rectangular surface may be expressed as the product of a function $f(x)$ and a function $f(y)$, then the directional pattern is the product of two patterns in planes containing the normal to the surface and parallel to the x and y axes, respectively. The full significance of this theorem will appear later when we discuss rectangular arrays of elements.

Since we have already shown that patterns in the principal planes of a rectangular array of point sources can each be given by a line of point sources, we shall consider an equally spaced, in-phase line of sources. The symbols that shall be used for such arrays are shown in Figure 3. The incident sound wave meets the line array at the angle θ as shown. All phases shall be referenced to that of the signal received by an element at the origin whether one is actually there or not. Note the right-left symmetry of the signal amplitudes.

Figure 4 is a representation of the signals recieved by each of the elements in a six element line array where $u = \frac{\pi d}{\lambda} \sin \theta$. The vectors above the axis represent the signals received from the elements on the right and those below the axis, the signals from the left.

It is easily seen from Figure 4 that the sum pattern of the six element line source is given by,

$$P_{\sigma 6} = A_1 \cos u + A_2 \cos 3u + A_3 \cos 5u \qquad (3)$$

and that over the major lobe the phase of the entire line array is the same as that of the reference signal. As θ and consequently u increases, $P_{\sigma 6}$ will at one point become zero (a null in the pattern) and then the phase suddenly reverses to 180°. Further increases of θ and u produce more nulls and phase reversals.

Figure 4 also shows that the difference pattern is given by,

$$P_{\delta,6} = A_1 \sin u + A_2 \sin 3u + A_3 \sin 5u \quad .$$

In this case, we note that for small angles of incidence on the right the phase leads by 90° and on the left lags by 90°. Whereas the sum pattern is a maximum for $\theta = 0$, the difference pattern is a null.

Corresponding pattern functions for odd number of elements are:

$$P_{\sigma n} = A_0 + A_1 \cos 2u + A_2 \cos 4u + \ldots$$

$$P_{\delta n} = A_1 \sin 2u + A_2 \sin 4u + \ldots$$

The characteristics of $P_{\sigma,6}$ and $P_{\delta,6}$ are illustrated in Figure 5. The combined use of these patterns give the necessary information for locating underwater targets. Note that over a range of incident angles near 0°, the difference between the magnitudes of the sum and difference patterns increases nearly linearly with θ. If the difference pattern leads the sum pattern by 90°, the target is on the right and if it lags by 90°, the target is on the left. In practice, the difference pattern is usually phase shifted 90° so that it is in phase for targets on one side and out of phase for the other.

It must be emphasized that those phase relationships hold only over a relatively small range of incident angles on both sides of the normal. In the minor lobe regions we noted earlier that phase reversals occur as θ is varied and where they occur are not the same for both patterns. Consequently, minor lobes, unless drastically reduced, will give false information. For

these reasons and others, methods for reducing minor lobes have been developed which are known as tapering or shading the array. It consists of a systematic variation of the signal amplitude coefficients of the elements. The process will be illustrated by an application to the six element array illustrated above.

Note that the pattern function was given by

$$P_{\sigma 6} = A_1 \cos u + A_2 \cos 3u + A_3 \cos 5u \qquad (3)$$

which is a Fourier series. This suggested the use of a Fourier transform relating the source strengths of the array to the pattern function. In one application, an amplitude distribution was derived to provide the Gaussian pattern. In this case, the Fourier transform is itself a Gaussian function.

However, the most common method of tapering is that developed by Dolph (Reference 2) and generally known as the Dolph-Chebyshev method because it sets the pattern function above equal to an appropriate Chebyshev polynomial.

In Equation (3) above, we let $x = \cos u$ and then express the cosine functions in powers of x using Chebyshev polynomials. Thus, Equation (3) becomes

$$\begin{aligned} P_{\sigma,6} &= A_1 x + A_2(4x^3 - 3x) + A_3(16x^5 - 20x^3 + 5x) \\ &= 16A_3x^5 + (4A_2 - 20A_3)x^3 + (A_1 - 3A_2 + 5A_3)x \quad . \end{aligned} \qquad (4)$$

The use of Chebyshev polynomials above is somewhat trivial compared to the really significant use which is to set the array polynomial above equal to

the Chebyshev polynomial

$$T_5(x_o x) = 16x_o^5 x^5 - 20x_o^3 x^3 + 5x_o x \qquad (5)$$

where $x_o > 1$ and is given by $x_o = \cosh\{\frac{1}{n}\cosh^{-1} r\}$ (6)

where $r = \frac{\text{major}}{\text{minor}}$ lobe ratio.

The amplitudes A_1, A_2 and A_3 are now easily calculated by equating coefficients of like powers of Equations (4) and (5).

Figure 6 illustrates the properties of the fifth degree Chebyshev polynomial which applies to the six element array. Over the range of $-1 \leq x_o x \leq 1$, the Chebyshev polynomial function ranges between ± 1 because in this range the function is limited to the cosine function. However, by extending the independent variable $x_o x$ beyond ± 1, the Chebyshev polynomials can take values to $\pm$ infinity. Thus, we can make $x_o x$ and consequently $T_5(x_o x)$ as large as possible. $T_5(x_o x)$ will then correspond to the peak or maximum of our response. On the other hand, the minor lobes will all be the same and equal to unity.

This design method is optimum in the sense that, for a given minor lobe reduction, one obtains the narrowest possible beamwidths for the equally spaced, in-phase elements at a given frequency. We design so that at $\theta = 90°$, the Chebyshev polynomial is of unity magnitude just beyond the last null.

There are relatively narrow limits on the range of element spacing. If the spacing is too large, e.g., greater than λ, a second major lobe would appear before $\theta = 90°$. Also, the method does not work if the spacing is much less than $\lambda/2$. For smaller spacings, a slightly different method

was introduced by Riblet (Reference 3) and extended by Pritchard (Reference 4). In this method which can be applied to an odd number of elements, a Chebyshev polynomial in terms of an angle $\phi = \frac{2\pi d}{\lambda} \sin\theta$ is used instead of $u = \frac{\pi d}{\lambda} \sin\theta$. This analysis leads to narrower patterns than those given by the Dolph-Chebyshev technique and are called super-directive arrays. However, as the spacing becomes smaller, some of the excitation amplitudes become negative, that is, out of phase with the others. For very small spacing, the sum is considerably less than the sum of absolute values. Smaller tolerances on the amplitudes are then generally required and over-all efficiency is decreased.

Some characteristics of the Dolph-Chebyshev patterns can be determined directly from the values of x_o, d and λ. Of course, the latter depends on the frequency. These characteristics are (1) maximum allowable spacing, and (2) beam width at any specified levels below the peak. These results are shown in Figure 7. Our experience with transducer elements cemented to a rubber pad and mounted in a housing showed that since there is a baffle effect that significantly reduces levels at incident angles beyond 70°, it was possible to design for the last minor lobe to occur around 70°. The dashed line indicates the extension of this tolerance.

We shall now illustrate the calculations of the excitation amplitudes for our six element array. If we design for a 30 dB minor lobe reduction, 20 log r will be set equal to 30, which gives $r = 31.6$. From Equation (6) we get a value of 1.35 for x_o. From Equations (4) and (5) we obtain the following values for A_N.

$A_1 = 15.60 \qquad A_2 = 10.70 \qquad A_3 = 4.66$

normalized $A_1 = 1.000 \qquad A_2 = 0.685 \qquad A_3 = 0.298$

Figure 8 illustrates how these values are used to extend the line array design to that for a two dimensional array using Equation (2). Due to the symmetry, only one quadrant of the array is necessary. Figure 9 gives the normalized values for these elements. Frequently the outside corner element is deleted so as to confirm to a circular housing. The pattern deterioration is generally small but in any case its effect is easily calculated. The numbers in parentheses give one possible set of turns on magnetostrictive stacks or on the transformer secondaries used with electric coupled transducer elements.

The coefficients that provide an optimum sum pattern are unsuitable for an optimum difference pattern. In fact, they degrade the difference pattern. Consequently, the difference pattern must be independently optimized.

With a slight modification, the Dolph technique may be employed to optimize a difference pattern, i.e., where the two halves are in phase opposition. The difference pattern function,

$$P_{\delta,6} = A_1 \sin u + A_2 \sin 3u + A_3 \sin 5u$$

may be expanded in terms of $\sin u$ as follows:

$$P_{\delta,6} = A_1 \sin u + A_2(3 \sin u - 4 \sin^3 u) + A_3(5 \sin u - 20 \sin^3 u + 16 \sin^5 u)$$

Now, if we divide by $\sin u$, we get,

$$\frac{P_{\delta,6}}{\sin u} = A_1 + A_2(3 - 4 \sin^2 u) + A_3(5 - 20 \sin^2 u + 16 \sin^4 u) \quad .$$

If we substitute $1 - \cos^2 u$ for $\sin^2 u$ and x for $\cos u$, the expression

above becomes,

$$\frac{P_{\delta,6}}{\sin u} = (A_1 - A_2 + A_3) + (4A_2 - 12A_3)\, x^2 + 16A_3 x^4 \quad .$$

We now equate this relationship to a 4th degree Chebyshev polynomial and proceed as before with the sum pattern. Please recall, however, that we used a 5th degree polynomial for the sum pattern. Also, note that since $P_{\delta,6} = \sin u\, T_4(x_o x)$, it is zero at $\theta = 0$ and then the absolute value increases rapidly for moderately small values of θ on both sides of zero.

The use of Equation (2) to extend the line array to a plane is shown in Figure 10. Here, the B factors are just the excitation coefficients for an optimum sum pattern. In fact, if all elements were connected in phase, we would obtain an optimum vertical sum pattern, but when the right and left halves are connected in phase opposition, we obtain the optimum horizontal difference pattern.

Figure 11 gives relative source amplitudes for the optimum difference pattern. The distinct difference between these coefficients and those for the sum pattern is quite evident by noting that the elements in the second column now have the greatest excitation instead of the first column as in the case of the sum pattern.

No direct method of finding x_o was available for the difference pattern but minor lobe reductions could be calculated for assumed values of x_o (see Reference 1) and plotted as shown in Figure 12. Thus, these plots permit us to select the appropriate x_o for a given minor lobe reduction.

Figure 5 presents a linear plot of the optimum sum and difference patterns. When this method for the optimum difference pattern was developed, it appeared that it would apply only to an even number of array columns. However, Geoffrey Wilson (Reference 5) has shown that it can be applied to

an odd number of columns, in which case the central column simply is not used to form the difference pattern.

Figure 13 is of academic interest. It represents the locus of the resultant signal from 1/2 of a transducer designed for (a) an optimum sum pattern and (b) an optimum difference pattern. It is the resultant of the vectors shown in Figure 4. The sum pattern response is the projection on the x-axis and that of the difference pattern is the projection on the y-axis. It clearly shows why the minor lobes are so small.

Tilted beams and end-fire arrays are obtained by introducing delay lines or phase shift networks into the circuits of each element or maybe column or row of the array so that for a given specified direction, the outputs of signals (including delays or phase shifts) will be in phase. The tapering procedures are generally similar to those described earlier.

Most of the development for end-fire arrays (beam tilted to 90°) resulted in superdirective arrays with some characteristics similar to those of Riblet (Reference 3) and Pritchard (Reference 4).

A somewhat different approach to the production of tilted sum and difference patterns was developed by W. J. Hughes and W. Thompson, Jr. (Reference 6). I shall demonstrate its use by an application to a tilted sum pattern which may be written,

$$P_\sigma = A_1 \cos(u - \phi) + A_2 \cos 3(u - \phi) + A_3 \cos 5(u - \phi) + \ldots$$

where ϕ is the required phase delay for elements on one side of center and phase advance for elements on the other side. Using the trigonometric identity for the cosine of the difference of two angles, the equation above becomes,

$$P_\sigma = [A_1 \cos \phi \cos u + A_2 \cos 3\phi \cos 3u + A_3 \cos 5\phi \cos 5u + \ldots]$$
$$+ [A \sin \phi \sin u + A_2 \sin 3\phi \sin 3u + A_3 \sin 5\phi \sin 5u + \ldots] .$$

Now for a given tilt angle ϕ, the sines and cosines involving ϕ are constants. Therefore, the pattern function becomes

$$P_\sigma = [A_1' \cos u + A_2' \cos 3u + A_3' \cos 5u + \ldots]$$
$$+ [A_1'' \sin u + A_2'' \sin 3u + A_3'' \sin 5u + \ldots]$$

where $A_n' = A_n \cos \phi$, and $A_n'' = A_n \sin \phi$, etc.

We note that P_σ is now the sum of a sum pattern and a difference pattern. Since the latter is in phase quadrature with the former, it must be shifted 90° before combining the two. Although the method is applicable to any values of A_m, tapering is easily achieved. The unprimed A_n coefficients are determined as before by using Chebyshev polynomials. The Hughes - Thompson technique is also applicable to tilted, difference patterns and end fire arrays. It is interesting to note that all pattern tapering techniques discussed so far have used Chebyshev polynomials.

An array tapering for an entirely different purpose was developed by W. J. Trott (Reference 7). Its purpose was to provide plane waves in a region of the near field of a relatively large array in order to calibrate transducers in the near field.

It is well known that the intensity along the axis of a circular radiating piston whose diameter is large compared to the wavelength has numerous maxima and minima (actually nulls) in the near field. It is also known that the total number of side lobes appearing in the far field is just twice the number of maxima which occur directly in front of the piston.

The above remarks suggest that if minor lobes are eliminated or greatly reduced, this axial variation should likewise be eliminated or reduced. Indeed this is the case. Applying these principles, Trott adjusted the excitation amplitudes of a large array of elements in order to provide an essentially plane wave region directly in front of the array. In his example, a 100 cm diameter array provided a cylindrical space in front of the array about 50 cm in diameter and about the same in length wherein there were plane waves.

Although it was not expressly stated, all the previous discussion was based on linear acoustic waves. When very intense, so-called finite sound waves are projected, non-linear or distorted waves are produced with a whole host of interesting properties. For example, if two pure tones are projected into the same medium, harmonics of the waves are produced, as well as sum and difference frequency waves. The highly directive character of these difference frequency beams was first recognized by Peter J. Westervelt (Reference 8).

In the following discussion we are primarily interested in the difference frequency that develops in the projected acoustic field. Usually the frequencies of the high intensity primary waves are close together so that the difference frequency is much smaller, say one-tenth or less.

When the near field primary wave absorption is quite small, the interaction zone will extend beyond the mean Rayleigh distance r_o . The interaction zone is that region in front of the transducer face where wave distortion occurs and acoustical energy is pumped from the primary waves into the distortion waves, including the difference frequency wave. Since this latter is of much lower frequency than any of the other waves and consequently attenuated much less than the others, it usually will be transmitted to greater ranges than the others even though its equivalent field pressure is much below that of the primary waves. The so-called

pumping occurs until the spreading loss of the primary waves reduce the intensity to such a level that distortion no longer exists. Since the virtual sources that produce the difference frequencies are essentially limited to the main beams of the primary waves, the low frequency difference pattern will be essentially the same as those of the much higher frequency primary patterns or even a little sharper. In fact, its far field directivity response is essentially equal to the product of the directivity responses of the primary patterns. One very important consequence of this is the almost total absence of minor lobes in the difference frequency pattern.

In order to achieve the same directivity with a conventional source operating at the difference frequency, the source diameter would have to exceed the diameter of the parametric array by the ratio of the mean primary frequency to the difference frequency.

The bandwidth of the difference frequencies may be very broad because it is really determined by the Q of the transducer that projects the primary waves.

Somewhat similarly, difference frequency waves can be produced which have a constant beam width over very wide frequency bands (e.g., greater than two octaves). Of course, sum, difference and tilted beams can be produced.

When the absorption coefficient of the primary waves is large, the attenuation may be so great that all of the interaction may take place within the near-field of the transducer, i.e., at ranges less than r_o. In this case, the interaction is essentially confined to a cylinder whose diameter is that of the transducer radiating face and of length roughly determined by the absorption coefficient. This interaction zone is really an extension of the source itself. Indeed, the beam-width of this virtual

end-fire array is given by the same relationship as that for an end-fire array and is always less than that for the "spreading-loss-limited" case.

Parametric receiving arrays are formed in a fluid by projecting a finite-amplitude "pump wave" into the medium to serve as a "carrier" for the weak incoming signal whose frequency equals the difference frequency of the transmitted waves.

REFERENCES

1. V. M. Albers, Underwater Acoustics Handbook II, The Pennsylvania State University Press, University Park, Penna., 1965.

2. C. L. Dolph, Inst. Radio Engrs. 34, 335-348, 1946.

3. H. J. Riblet, Proc. Inst. Radio Engrs. 35, 489-492, 1947.

4. R. L. Pritchard, J. Acoust. Soc. Am. 25, 879-891, 1953.

5. G. L. Wilson, J. Acoust. Soc. Am. 34, 915, 1966.

6. W. J. Hughes and W. Thompson, Jr., J. Acoust. Soc. Am. 59, 1040-1045, 1976.

7. W. J. Trott, J. Acoust. Soc. Am. 36, 1557-1568, 1964.

8. P. J. Westervelt, J. Acoust. Soc. Am. 32, 934, 1960.

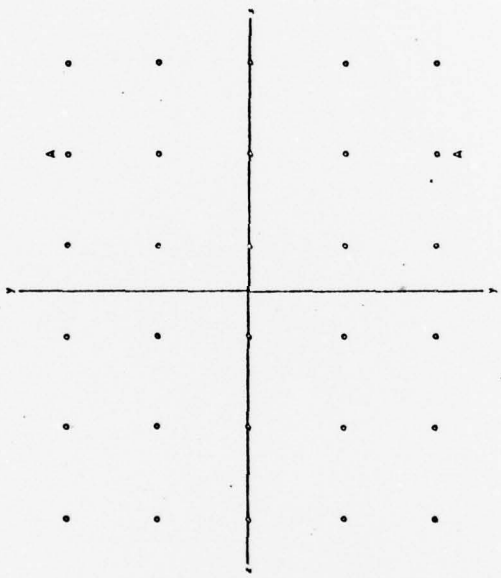

Figure 1 - Plane array of point sources showing the arrangement in rows and columns.

LINE SOURCE

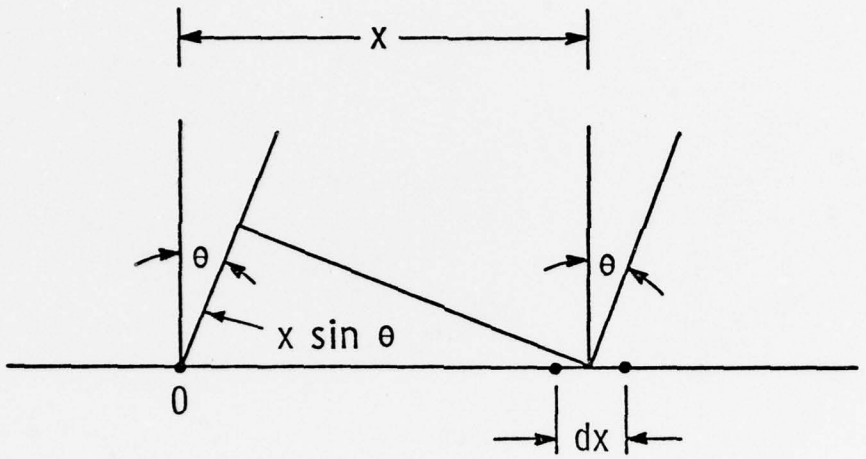

$$\psi = \frac{2\pi x}{\lambda} \sin\theta = kx \sin\theta$$

ψ: PHASE
λ: WAVELENGTH

Figure 2

July 7, 1977
PMK:cdn

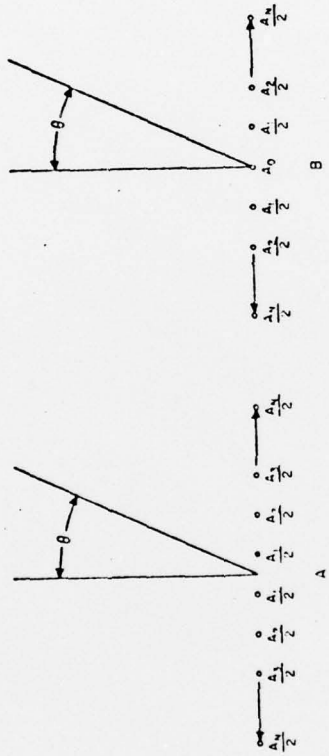

Figure 3 - Symbols for equally spaced linear arrays of point sources; (A) even number of sources, (B) odd number of sources.

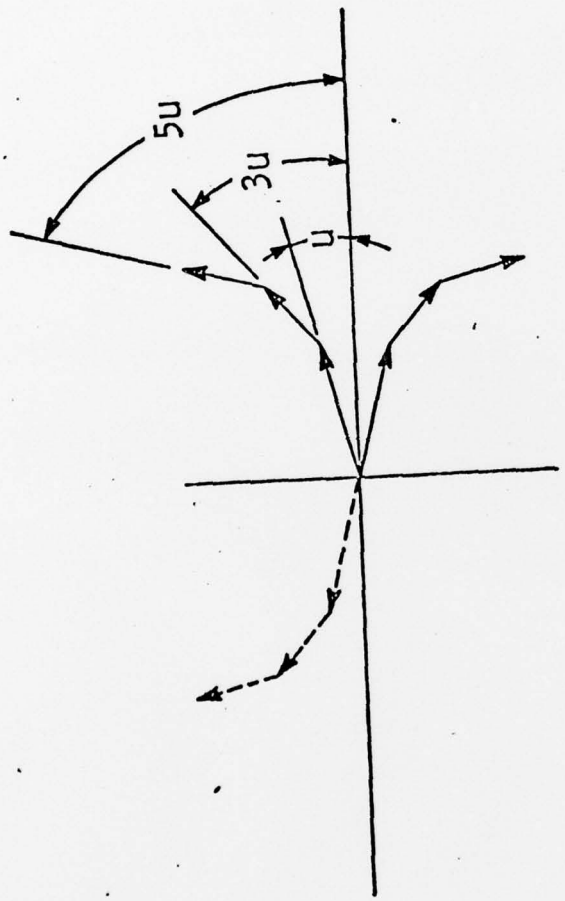

Figure 4. Vector Representation of Sum and Difference Responses

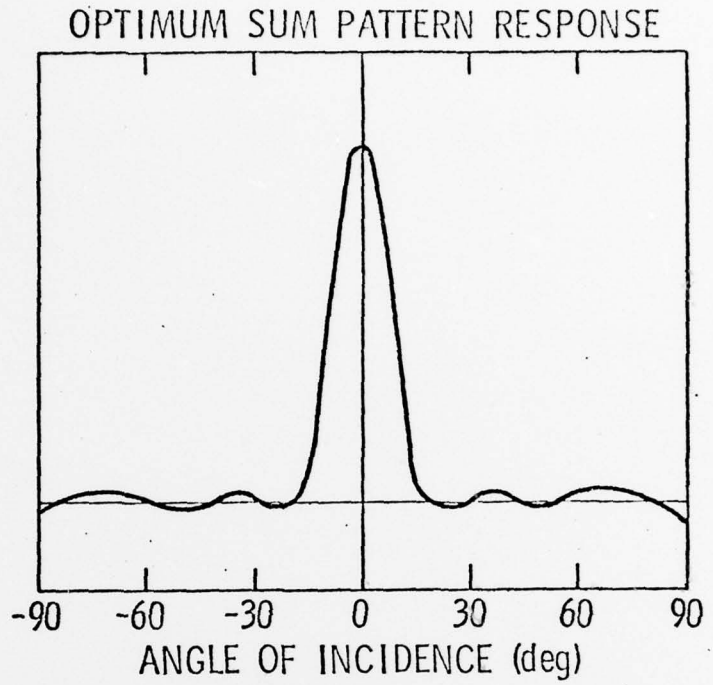

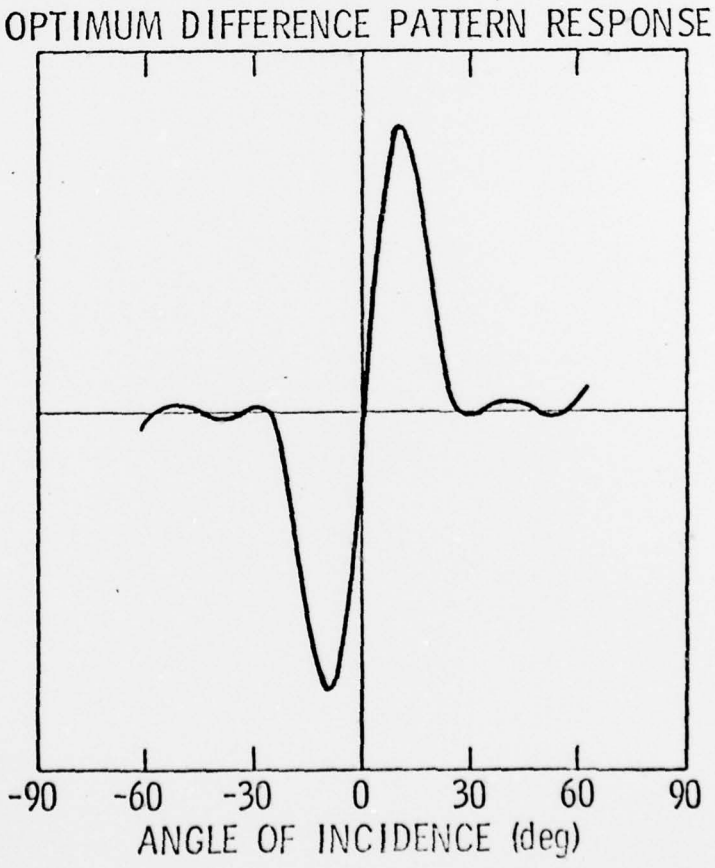

Figure 5 - Sum and difference responses

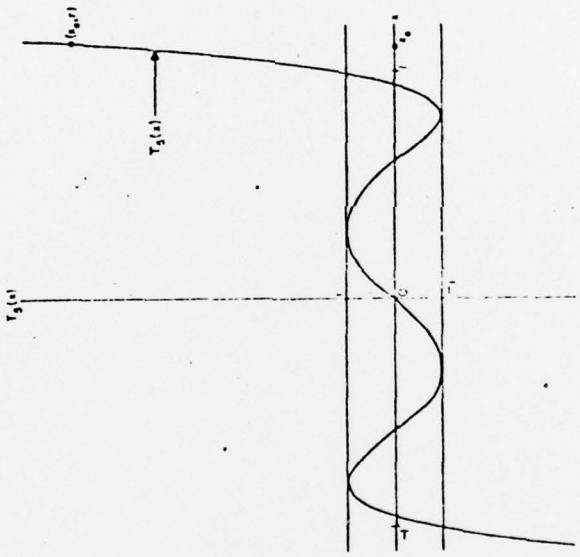

Figure 6 - Fifth Chebyshev polynomial showing relationship between signal to noise ratio r and parameter x_o.

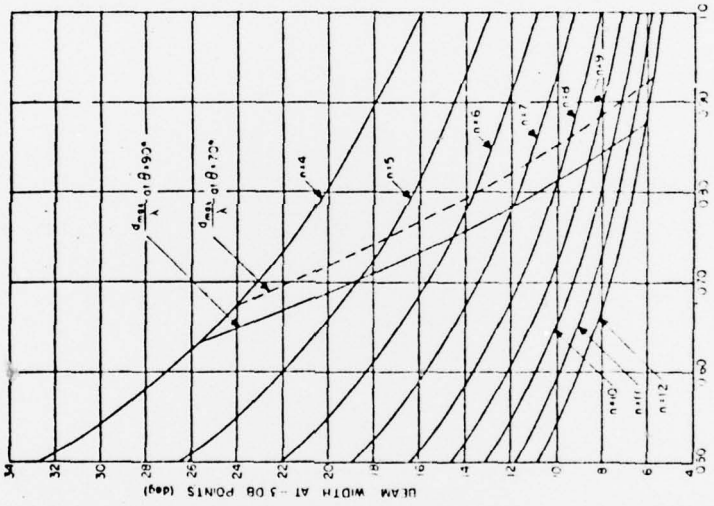

Figure 7 - Beam width vs. spacing for 30 db minor lobe reduction.
Parameter: number of elements.

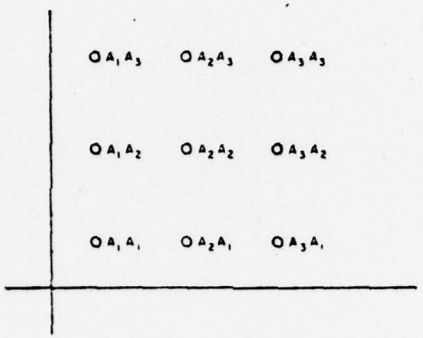

Figure 8 - Use of second product theorem to determine source amplitudes for a plane array sum pattern.

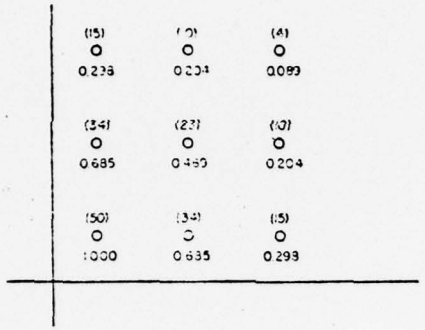

Figure 9 - Relative source amplitudes for a plane array designed for an optimum sum pattern. Numbers in parenthesis give one possible set of values for turns on magnetostrictive stacks.

July 7, 1977
PMK:cdn

Figure 10 - Use of second-product theorem to determine source amplitudes for the difference pattern of a plane array.

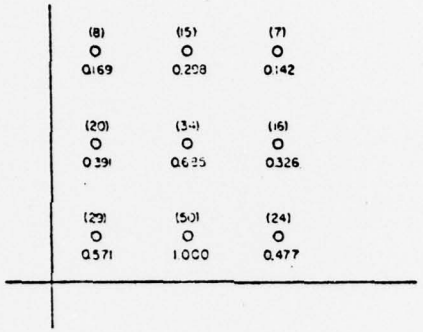

Figure 11 - Relative source amplitudes for a plane array designed for an optimum difference pattern. Numbers in parenthesis give one possible set of values for the turns on magnetostrictive stacks.

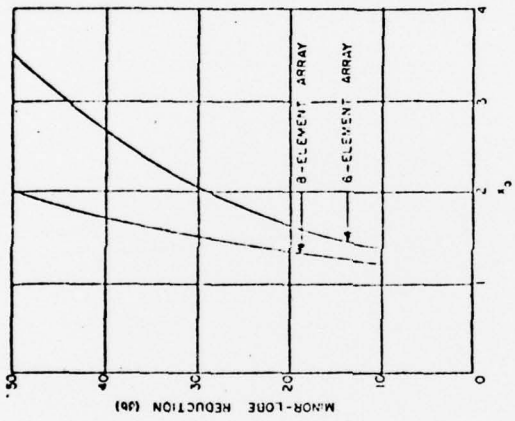

Figure 12 - Maximum minor lobe level relative to the level of the main beams for optimum difference patterns of six and eight element line arrays.

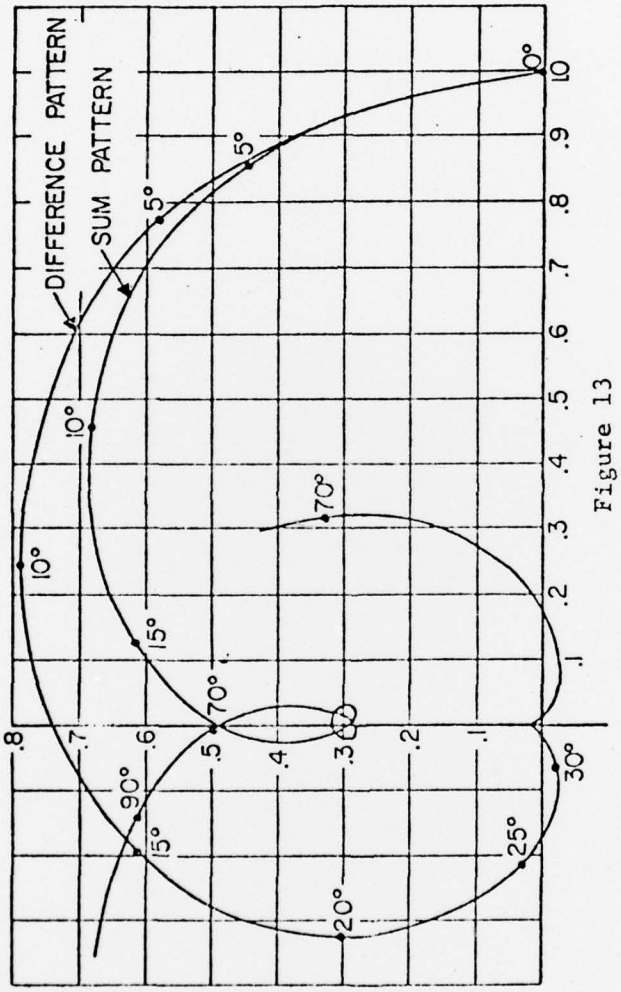

Figure 13

LOCUS OF VECTOR REPRESENTING THE SIGNAL FROM A HALF TRANSDUCER DESIGNED FOR (a) AN OPTIMUM SUM PATTERN AND (b) AN OPTIMUM DIFFERENCE PATTERN.

DISTRIBUTION LIST -- TM 77-213

NAVSEA, Dr. E. G. Liszka, SEA-03421, Copy No. 1
NAVSEA, Mr. T. E. Douglass, PMS 406E1, Copy No. 2
DDR&E, Dr. E. J. McKinney, Copy No. 3
NAVSEA, Code SEA-09G32, Copies No. 4 and 5
Picker Corp., 12 Clintonville Rd, Northford, CT 06472,
Mr. R. B. Bernardi, Copy No. 6
DDC, Copies No. 7 through 18